

# Some notes about scanning probe microscopy, nanoengineering and methods of quantum mechanics

A E Rassadin<sup>1</sup>, T S Sazanova<sup>1,2</sup>, A V Stepanov<sup>1,3</sup> and L A Fomin<sup>1,4</sup>

<sup>1</sup> Nizhny Novgorod Mathematical Society, Nizhny Novgorod, 603950, Russia

<sup>2</sup> Nizhny Novgorod State Technical University n.a. R.E. Alekseev, 603950, Nizhny Novgorod, Russia

<sup>3</sup> Chuvash State Agricultural Academy, 428000, Cheboksary, Russia

<sup>4</sup> Institute of Microelectronics Technology and High Purity Materials RAS, 142432, Chernogolovka, Moscow region, Russia

brat\_ras@list.ru

**Abstract.** In the presented paper, a research program for new vision of nanoengineering has been suggested. In the framework of this program, growth of a solid state surface under the influence of external source of sputtering particles is considered as the problem of optimal control by distributed parameter system, the source being a control. As one of cornerstones in this approach, general theory of the one-dimensional KPZ-equation in approximation of small angles under the action of the spatially-inhomogeneous source has been developed. The complete mathematical model of this process with the Dirac delta function source of external particles illustrates this theory, Green's function for this system having been calculated exactly. Scheme of physical realization of delta-functional source by means of series of carbon nanotubes has been discussed. Opportunity of combined characterization of solid state surface by both atomic force microscopy and scattering data for electromagnetic waves has been demonstrated. The height of the sample has been constructed with help of the Cole-Hopf substitution from single eigenfunction of discrete spectrum being an example of the surface shape under investigation.

## 1. Introduction

From 1981 to 2018, scientific community all over the world has been witnessing intensive development of scanning probe microscopy [1]. Nowadays, various modes of scanning probe microscopy have covered different spheres of contemporary material science – from the use of magnetic force microscopy for the research of epitaxial ferro- and antiferromagnetic structures [2] to the application of atomic force microscopy for the study of chitosan's and chitosan-based copolymers' mechanical properties [3]. In particular, the increase of precision for measurements using atomic force microscopy proves to give us an opportunity of verification of different models for growth of solid state surfaces [4].

At present, the most popular model of such kind is the Kardar-Parisi-Zhang equation (KPZ) [5]:

$$\frac{\partial H}{\partial t} = c \cdot \sqrt{1 + (\nabla H)^2} + \nu \cdot \nabla^2 H + U(\vec{x}, t) \quad (1)$$

This phenomenological equation describes temporal evolution of the height  $H(\vec{x}, t)$  of solid state surface under sputtering of a substance on it,  $\vec{x} = (x_1, x_2)$  being two-dimensional vector and  $\nabla$  being two-dimensional gradient. The first term on the right-hand side of the KPZ-equation demonstrates that



the growth of the surface occurs only along the local normal  $\vec{n}(\vec{x}, t) = \left( \frac{-\nabla H}{\sqrt{1 + (\nabla H)^2}}, \frac{1}{\sqrt{1 + (\nabla H)^2}} \right)$  to

it, rate  $c$  of this growth being constant. The second term on the right-hand side of the equation (1) corresponds to the surface diffusion of sputtering substance,  $\nu$  being a diffusion coefficient. Moreover, this term regularizes the input equation preventing a gradient catastrophe, which might be generated by the presence of the first term only. The third term  $U(\vec{x}, t)$  is the external source of sputtering particles. It is obvious that at arbitrary moment of time  $t \geq 0$  this function ought to be nonnegative everywhere:  $U(\vec{x}, t) \geq 0$ . As a rule, the Cauchy problem for the equation (1) is studied:

$$H(\vec{x}, 0) = h_0(\vec{x}), \quad \vec{x} \in D \subset R^2, \quad (2)$$

initial condition being corresponded to initial shape of the surface under consideration.

For instance, the KPZ-equation proves to be highly adequate to the physical experiment during the simulation of manufacturing process of multilayer mirrors and gratings employed in X-ray optics [6]; therefore, verification procedure for model (1) of the surface growth with support of this one by means of atomic force microscopy is not required. The situation gives rise to the problem of uncertainty under choice of direction of further epistemological movement. Nevertheless, there is the way to overcome this obstacle by considering the external source of particles  $U(\vec{x}, t)$  as a control. At last, in this case the equation (1) ought to be added by demand of minimization of some functional of height  $H(\vec{x}, t)$  and control  $U(\vec{x}, t)$ :

$$F[H, U] = \int_0^T \int_D f(H(\vec{x}, t), U(\vec{x}, t)) d^2x dt \rightarrow \min \quad (3)$$

Conditions (1)-(3) form the problem of optimal control by distributed parameter system [6]. Namely, starting from the initial shape  $h_0(\vec{x})$  by means of control  $U(\vec{x}, t)$  it is required to achieve minimum of functional (3) on the fixed interval of time  $[0, T]$ . For example, one can set up the problem of the closest fitting of fixed shape  $H_*(\vec{x})$  by height  $H(\vec{x}, T)$  at the moment of time  $t = T$  in  $L^2(D)$ -metric:

$$\int_D [H(\vec{x}, T) - H_*(\vec{x})]^2 d^2x \rightarrow \min \quad (4)$$

We stress that on the interval  $[0, T]$  of time function  $H(\vec{x}, t)$  must obey to the equation (1). In other words, it is the problem of nanoengineering.

The first obvious solution of this problem is to apply the infinite-dimensional generalization of Pontryagin's maximum principle [8]. In order to reduce the KPZ-equation to infinite-dimensional dynamical system in the space  $l_2$  of square-summable sequences of complex numbers, let us expand functions  $H(\vec{x}, t)$  and  $U(\vec{x}, t)$  on an orthonormal basis  $\{\Phi_n(\vec{x})\}_{n=0}^{\infty}$  in separable Hilbert space  $L^2(D)$ :

$$H(\vec{x}, t) = \sum_{n=0}^{\infty} h_n(t) \cdot \Phi_n(\vec{x}), \quad U(\vec{x}, t) = \sum_{n=0}^{\infty} u_n(t) \cdot \Phi_n(\vec{x}) \quad (5)$$

denumerable sets of Fourier coefficients  $h_n(t)$  and  $u_n(t)$  representing dynamical variables in  $l_2$  and controls therein, respectively. But the substitution of the first Fourier-series expansion from (5) into the equation (1) ends in failure, because the strong nonlinearity of this equation does not allow obtaining any visible result. This circumstance demonstrates that to do the step forward, one must simplify the KPZ-equation in the framework of the conjecture about correctness of the inequality  $|\nabla H| \ll 1$  using the so-called approximation of small angles [5]. The result of this simplification is equal to:

$$\frac{\partial H}{\partial t} = c + \frac{c}{2} \cdot (\nabla H)^2 + \nu \cdot \nabla^2 H + U(\vec{x}, t) \quad (6)$$

Further, let us introduce a new unknown function  $\varphi(\vec{x}, t)$  as follows:

$$H(\vec{x}, t) = c \cdot t + \frac{2 \cdot \nu}{c} \cdot \ln \varphi(\vec{x}, t) \quad (7)$$

The expression (7) is known to be the Cole-Hopf substitution [5]. By means of this formula, one can reduce the nonlinear equation (6) to the Cauchy problem for the next one:

$$\frac{\partial \varphi}{\partial t} = \nu \cdot \nabla^2 \varphi + \frac{c \cdot U(\vec{x}, t)}{2 \cdot \nu} \cdot \varphi, \quad \varphi(\vec{x}, 0) = \exp\left[\frac{c \cdot h_0(\vec{x})}{2 \cdot \nu}\right] \quad (8)$$

The linear parabolic equation (8) is simpler than the nonlinear equation (6).

For the functional (4) it is interesting to consider two-stage control:

$$U(\vec{x}, t) = \begin{cases} Q(\vec{x}, t), & 0 \leq t \leq T \\ 0, & t > T \end{cases} \quad (9)$$

where positive value  $T$  being fixed.

The formula (9) describes the situation of free evolution of the system (6) under  $t > T$ . If  $t > T$ , then the second term on the right-hand side of the equation (8) disappears and this equation is transformed into a trivial two-dimensional diffusion equation:

$$\frac{\partial \varphi}{\partial t} = \nu \cdot \nabla^2 \varphi \quad (10)$$

Let us assume that on the interval of time  $[0, T]$  there is a control  $Q_*(\vec{x}, t)$ , under which global minimum of the functional (4) would be achieved that is  $H(\vec{x}, T) = H_*(\vec{x})$  almost everywhere in the region  $D$ . Hence, further evolution of height can be described by means of Green's function of the equation (10) [9] and the Cole-Hopf substitution (7):

$$H(\vec{x}, t) = c \cdot (t - T) + \frac{2 \cdot \nu}{c} \cdot \ln \left( \int_{R^2} \exp \left[ -\frac{(\vec{x} - \vec{\xi})^2}{4 \cdot \nu \cdot (t - T)} + \frac{c \cdot H_*(\vec{\xi})}{2 \cdot \nu} \right] \cdot \frac{d^2 \xi}{4 \cdot \pi \cdot \nu \cdot (t - T)} \right) \quad (11)$$

For example, if the fixed shape  $H_*(\vec{x})$  is equal to:

$$H_*(\vec{x}) = \frac{2 \cdot \nu}{c} \cdot \ln \left[ \left( 1 + m_0 \cdot \cos \frac{2 \cdot \pi \cdot x_1}{a} \right) \cdot \left( 1 + m_0 \cdot \cos \frac{2 \cdot \pi \cdot x_2}{a} \right) \right] \quad (12)$$

then under  $t > T$  the formula (11) gives us [10]:

$$H(\vec{x}, t) = c \cdot (t - T) + \frac{2 \cdot \nu}{c} \cdot \ln \left[ \left( 1 + m(t) \cdot \cos \frac{2 \cdot \pi \cdot x_1}{a} \right) \cdot \left( 1 + m(t) \cdot \cos \frac{2 \cdot \pi \cdot x_2}{a} \right) \right] \quad (13)$$

where  $0 < m_0 < 1$ ,  $m(t) = m_0 \cdot \exp(-4 \cdot \pi^2 \cdot \nu \cdot t / a^2)$  and  $a$  is the lattice constant.

The explicit solution (13) may be interpreted as surface of crystal with cubic symmetry growing in the direction of one of the primitive translation vectors. At each moment of time  $t > T$ , this function is homothetic to the initial condition (12) for it. Graph of function (12) is presented in Figure 1.

It is well known that besides Pontryagin's maximum principle [8], there exist quite a few alternative approaches to solving problems of optimal control by distributed parameter systems ([7, 11-13] and references therein). On the other hand, to solve the problem defined by conditions (2), (4), (6), and (9) under  $t \in [0, T]$ , it is necessary to study a number of model situations in order to find the most convenient phase space for this problem. That is why in accordance with the classical sample [8] let us restrict area of our research by the next simplifications. Namely, we shall consider only surfaces with cylindrical generatrix (Fig. 2) and stationary controls depending on longitudinal coordinate only.

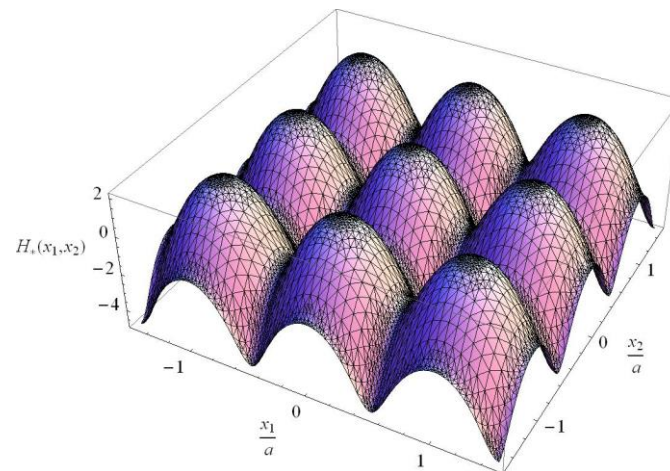


**Figure 1.** An example of the initial shape of the surface with convenient expression for its free evolution.

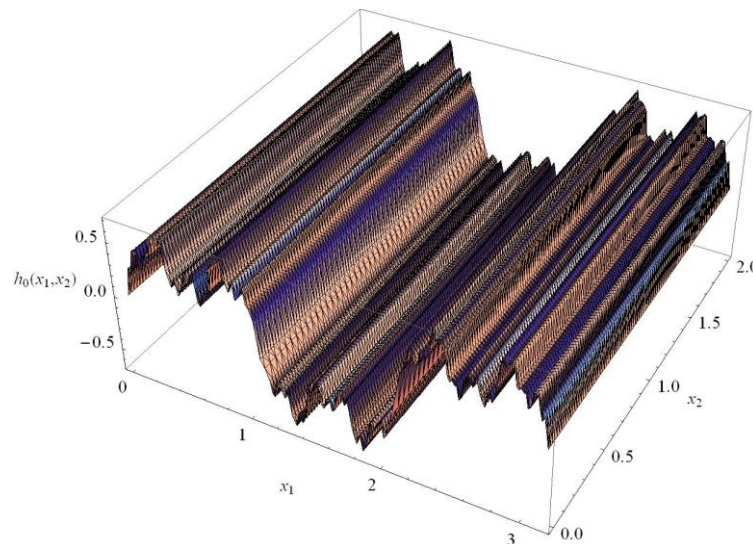


**Figure 2.** An example of a surface with a cylindrical generatrix.

The rest of the article is organized as follows: in Section 2 we demonstrate, how to construct a general solution of the one-dimensional KPZ-equation in approximation of small angles under the action of the spatially-inhomogeneous source  $Q(x)$ , which vanishes on infinity:  $\lim_{x \rightarrow \pm\infty} Q(x) = 0$ . Section 3 deals with

the case, when the source profile is proportional to the Dirac delta function:  $Q(x) = \frac{4 \cdot v^2 \cdot q}{c} \cdot \delta(x)$ . In

section 4 we consider both the simplest solution of the KPZ-equation with the delta-functional source and the approach to measurement of surface diffusion coefficient  $v$  along conducting surfaces by means of electromagnetic waves scattering. Final section is devoted to the discussion of results elaborated and perspectives of further investigations.

## 2. General theory of one-dimensional KPZ-equation with a spatially-inhomogeneous source

The aim of this section is to compare a number of methods to find the exact solution of the one-dimensional KPZ-equation in approximation of small angles with a time-independent external source  $Q(x)$ . In this case, the Cauchy problem for equation (6) is reduced to:

$$\frac{\partial H}{\partial t} = c + \frac{c}{2} \cdot \left( \frac{\partial H}{\partial x} \right)^2 + \nu \cdot \frac{\partial^2 H}{\partial x^2} + Q(x), \quad H(x,0) = h_0(x), \quad x \in R \quad (14)$$

The Cole-Hopf substitution (7) transforms the equation (14) to the next one:

$$\frac{\partial \varphi}{\partial t} = \nu \cdot \frac{\partial^2 \varphi}{\partial x^2} + \frac{c \cdot Q(x)}{2 \cdot \nu} \cdot \varphi, \quad \varphi(x,0) = \exp \left[ \frac{c \cdot h_0(x)}{2 \cdot \nu} \right] \quad (15)$$

This linear second-order parabolic partial differential equation might be solved in the framework of the newest technique developed in Ref. [14]. Exact solution of Eq. (15) can be expressed as follows:

$$\varphi(x,t) = \lim_{n \rightarrow \infty} \left[ \hat{S}^n \left( \frac{t}{n} \right) \cdot \varphi(x,0) \right] \quad (16)$$

where

$$\hat{S}(t) = ch^2 \left[ 2 \cdot \sqrt{\nu \cdot t} \cdot \frac{\partial}{\partial x} \right] + \frac{c \cdot t}{2 \cdot \nu} \cdot Q(x) \quad (17)$$

is the so-called space shift operator [14]. However, application of Eq. (16) under  $Q(x) \neq 0$  is very hard, because calculation of sequential degrees of the operator (17) under increase of exponent  $n$  in Eq. (16) becomes more awkward. On the other side, the exact solution of equation (15) can be represented as:

$$\varphi(x,t) = \int_{-\infty}^{+\infty} G(x,\xi;t) \cdot \varphi(\xi,0) \cdot d\xi \quad (18)$$

where  $G(x,\xi;t)$  is Green's function of this equation, which can be found by means of the Feynman-Kac formula [15, 16]:

$$G(x,\xi;t) = \int_{C(t,x-\xi)} \exp \left[ \frac{c}{8 \cdot \nu^2} \cdot \int_0^t Q(x + \eta(\tau)) \cdot d\tau \right] \cdot d_{W(t,x-\xi)} \eta \quad (19)$$

Path integral (19) is calculated on functional space  $C(t, x - \xi)$  of continuous on interval  $[0, \tau]$  functions  $\eta(\tau)$  obeying to the boundary conditions:  $\eta(0) = 0$  and  $\eta(t) = x - \xi$ . The symbol  $d_{W(t,x-\xi)} \eta$  designates the so-called conditional Wiener measure [15, 16]. But calculation of Green's function according to the Eq. (19) is quite difficult too; that is why let us find the solution of the linear Eq. (15) in the form:

$$\varphi(x,t) = \exp(-\nu \cdot \varepsilon \cdot t) \cdot \psi(x) \quad (20)$$

It is easy to check that a new unknown function  $\psi(x)$  obeys to the stationary Schrödinger equation:

$$\hat{H} \cdot \psi = \varepsilon \cdot \psi \quad (21)$$

with the Hamiltonian

$$\hat{H} = -\frac{d^2}{dx^2} + W(x) \quad (22)$$

where the role of potential energy is played by the function  $W(x) \equiv -\frac{c}{2 \cdot \nu^2} \cdot Q(x)$ . Due to nonnegativity and vanishing on infinity of the source  $Q(x)$ , the Hamiltonian (22) possesses both the discrete spectrum of negative eigenvalues  $\varepsilon_n$  ( $n = 0, N-1$ ) and the continuous spectrum of positive eigenvalues  $\varepsilon$  [17]. Green's function  $G(x,\xi;t)$  as a kernel of operator of evolution  $\exp(-\nu \cdot t \cdot \hat{H})$  for (15) is equal to:

$$G(x,\xi;t) = \sum_{n=0}^{N-1} \exp(-\nu \cdot \varepsilon_n \cdot t) \cdot \psi_n(x) \cdot \psi_n^*(\xi) + \int_0^{+\infty} \exp(-\nu \cdot \varepsilon \cdot t) \cdot \psi(x,\varepsilon) \cdot \psi^*(\xi,\varepsilon) \cdot d\varepsilon \quad (23)$$

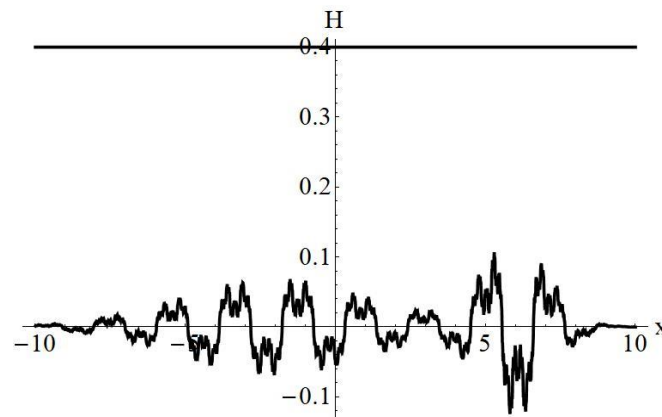


**Figure 3.** Initial shape (from below) and constant fixed shape (from above).

In the formula (23),  $N$  eigenfunctions of discrete spectrum  $\psi_n(x)$  and eigenfunctions  $\psi(x, \varepsilon)$  of continuous spectrum ought to be normalized according to standard rules of quantum mechanics [17]:

$$\int_{-\infty}^{+\infty} \psi_n^*(x) \cdot \psi_m(x) \cdot dx = \delta_{nm}, \quad \int_{-\infty}^{+\infty} \psi_n^*(x) \cdot \psi(x, \varepsilon) \cdot dx = 0, \quad \int_{-\infty}^{+\infty} \psi^*(x, \varepsilon) \cdot \psi(x, \varepsilon') \cdot dx = \delta(\varepsilon - \varepsilon') \quad (24)$$

Moreover, integrals (24) mean that the phase space  $L^2(R)$  of the system (15) is decomposed into direct sum of subspace  $V^d$  with basis from eigenfunctions of the discrete spectrum and subspace  $V^c$  with basis from eigenfunctions of the continuous spectrum:  $L^2(R) = V^d \oplus V^c$ .

Having found Green's function from the expression (23), we can return to investigation of the height  $H(x, t)$  using formulae (18) and (7). In the case under consideration, the functional (4) is reduced to:

$$\int_{-\infty}^{+\infty} [H(x, T) - H_*(x)]^2 dx \rightarrow \min, \quad (25)$$

and as a fixed shape one can choose the function  $H_*(x) = h_T \equiv \text{const}$  corresponding to uniformly flat surface. This situation is presented in Figure 3.

If on the interval of time  $[0, T]$  there is a control under which global minimum of the functional (25) would be achieved that is  $H(x, T) = h_T$  almost everywhere on  $R$  then under  $t > T$  evolution of the system (14) with the source  $Q(x) \equiv 0$  obeys to the next very simple expression:

$$H(x, t) = h_T + c \cdot (t - T) \quad (26)$$

The formula (26) claims that under  $t > T$  there is no roughness on the surface under investigation.

### 3. Surface with cylindrical generatrix under the action of the Dirac delta function source of sputtering particles

In this section, general theory developed in the previous section is applied to the source proportional to the Dirac delta function:  $Q(x) = \frac{4 \cdot v^2 \cdot q}{c} \cdot \delta(x)$ . In geometry with cylindrical generatrix this source can be physically realized by means of the channelling of slow atomic particles along the series of carbon nanotubes [18] situated on the straight line  $x = 0$ . This configuration is illustrated by Figure 4.

Thus, in this case Eq. (15) is equal to:

$$\frac{\partial \varphi}{\partial t} = v \cdot \frac{\partial^2 \varphi}{\partial x^2} + 2 \cdot v \cdot q \cdot \delta(x) \cdot \varphi \quad (27)$$

and the stationary Schrödinger equation (21) transforms to the following:

$$-\frac{d^2\psi}{dx^2} - 2 \cdot q \cdot \delta(x) \cdot \psi = \varepsilon \cdot \psi \tag{28}$$

This equation is known to describe the quantum mechanical problem about the delta-functional well [19]. In accordance with [19] under  $x \neq 0$  the equation (28) is reduced to the following one:

$$-\frac{d^2\psi}{dx^2} = \varepsilon \cdot \psi \tag{29}$$

which ought to be added by boundary conditions at  $x = 0$  [19]:

$$\psi(0+0) = \psi(0-0) \equiv \psi(0), \quad \frac{d\psi}{dx}(0+0) - \frac{d\psi}{dx}(0-0) + 2 \cdot q \cdot \psi(0) = 0 \tag{30}$$

It is easy to obtain from Eqs. (29) and (30) that in this system there is the unique state of the discrete spectrum:

$$\psi_0(x) = \sqrt{q} \cdot \exp(-q \cdot |x|) \tag{31}$$

corresponding to eigenvalue  $\varepsilon_0 = -q^2$  [19]. Graphs of potential well  $W(x) = -2 \cdot q \cdot \delta(x)$  and the normed ground state (31) in dimensionless coordinate are presented in Figure 5.

But our further construction sharply differs from this one in Ref. [19] because we take into consideration the next projection operator  $\hat{P}$  acting on arbitrary wave function  $\psi(x)$  as follows:

$$\hat{P} \cdot \psi(x) = \psi(-x). \tag{32}$$

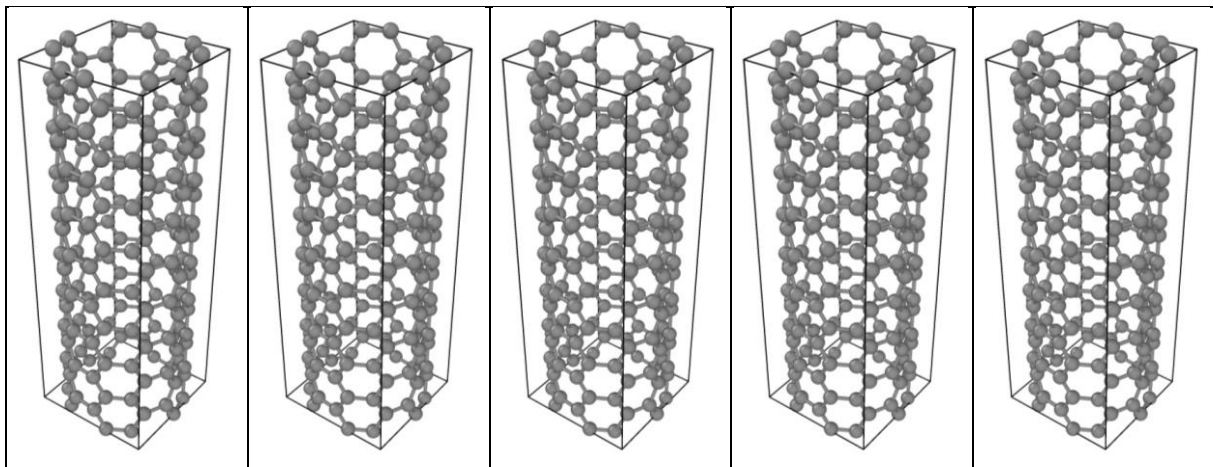


**Figure 4.** Series of carbon nanotubes as realization of delta-functional source.

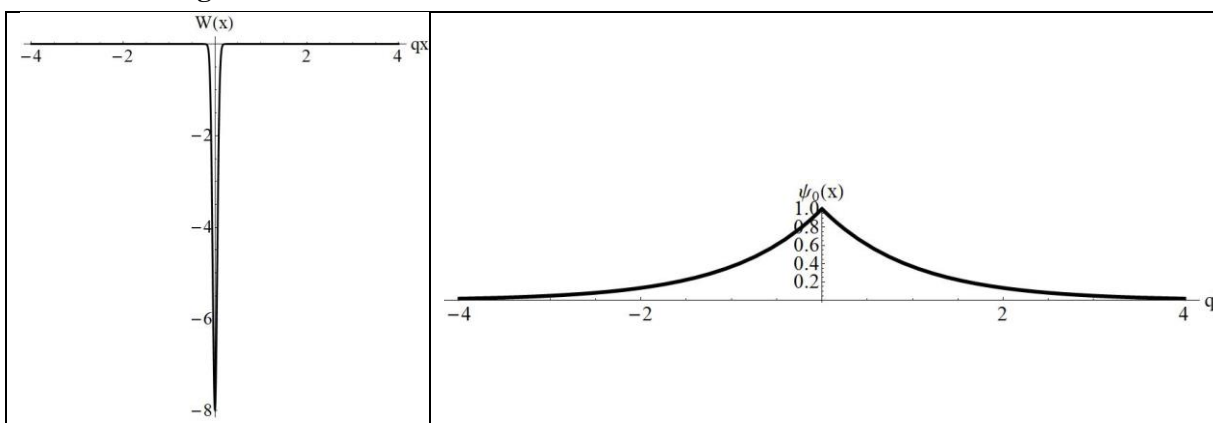


**Figure 5.** The delta potential well (on the left) and the ground state (on the right).

The Hermitian operator (32) is the well-known parity operator with eigenvalues  $P = \pm 1$  [17, 19].

The Hamiltonian of the problem  $\hat{H} = -\frac{d^2}{dx^2} - 2 \cdot q \cdot \delta(x)$  commutes with the parity operator:  $[\hat{H}, \hat{P}] = 0$ . Hence, for both of them there are common eigenfunctions [17, 19]:  $\hat{H} \cdot \psi_k^\pm = k^2 \cdot \psi_k^\pm$  and  $\hat{P} \cdot \psi_k^\pm = \pm \psi_k^\pm$ . Using Eqs. (29) and (30), one can establish that:

$$\psi_k^+(x) = \frac{1}{\sqrt{\pi}} \cdot \frac{k \cdot \cos(k \cdot x) - q \cdot \sin(k \cdot |x|)}{\sqrt{k^2 + q^2}}, \quad \psi_k^-(x) = \frac{1}{\sqrt{\pi}} \cdot \sin(k \cdot x) \quad (33)$$

Both of eigenfunctions (33) are normed on the Dirac delta function on  $k$ :

$$\int_{-\infty}^{+\infty} \psi_k^\pm(x) \cdot \psi_{k'}^\pm(x) \cdot dx = \delta(k - k') \quad (34)$$

and correspond to the same eigenvalue  $\varepsilon = -k^2$ . Graphs of functions (33) in dimensionless coordinate under  $k = \pi \cdot q$  are presented in Figure 6. Application of the general formula (23) for the delta potential well gives us the following expression for Green's function of the equation (27):

$$G(x, \xi; t) = \exp(\nu \cdot t \cdot q^2) \cdot \psi_0(x) \cdot \psi_0(\xi) + \int_0^{+\infty} \exp(-\nu \cdot t \cdot k^2) \cdot [\psi_k^+(x) \cdot \psi_k^+(\xi) + \psi_k^-(x) \cdot \psi_k^-(\xi)] \cdot dk \quad (35)$$

It is easy to check that for functions (31) and (33) the next relation is true:

$$\psi_0(x) \cdot \psi_0(\xi) + \int_0^{+\infty} [\psi_k^+(x) \cdot \psi_k^+(\xi) + \psi_k^-(x) \cdot \psi_k^-(\xi)] \cdot dk = \delta(x - \xi) \quad (36)$$

Therefore, Green's function (35) obeys to the standard initial condition:  $G(x, \xi; 0) = \delta(x - \xi)$ .

The result of calculation of Green's function in accordance with Eq. (35) is equal to:

$$G(x, \xi; t) = \frac{1}{2 \cdot \sqrt{\pi \cdot \nu \cdot t}} \cdot \exp\left[-\frac{(x - \xi)^2}{4 \cdot \nu \cdot t}\right] + \exp(\nu \cdot t \cdot q^2) \cdot [G_1(x, \xi; t) + G_2(x, \xi; t) + G_3(x, \xi; t)] \quad (37)$$

where

$$G_1(x, \xi; t) = q \cdot \exp(-q \cdot |x - q \cdot | \xi |) \quad (38)$$

$$G_2(x, \xi; t) = -\frac{\pi \cdot q}{4} \cdot [g(x + \xi, t) + g(-x - \xi, t) + g(x - \xi, t) + g(\xi - x, t)] \quad (39)$$

$$G_3(x, \xi; t) = \frac{\pi \cdot q}{4} \cdot [g(|x| - |\xi|, t) + g(|\xi| - |x|, t) + g(|x| + |\xi|, t) - 3 \cdot g(-|x| - |\xi|, t)] \quad (40)$$

Functions (39)-(40) express via the next auxiliary function connected with the complementary error integral:

$$g(\zeta, t) = \exp(q \cdot \zeta) \cdot \operatorname{erfc}\left(\frac{\zeta}{2 \cdot \sqrt{\nu \cdot t}} + q \cdot \sqrt{\nu \cdot t}\right) \quad (41)$$

Moreover, functions (38)-(40) are invariant under the action of the abelian point group  $C_4$  on the plane  $(x, \xi)$ .

Typical graph of Green's function (37) under fixed time  $t$  is presented in Figure 7.

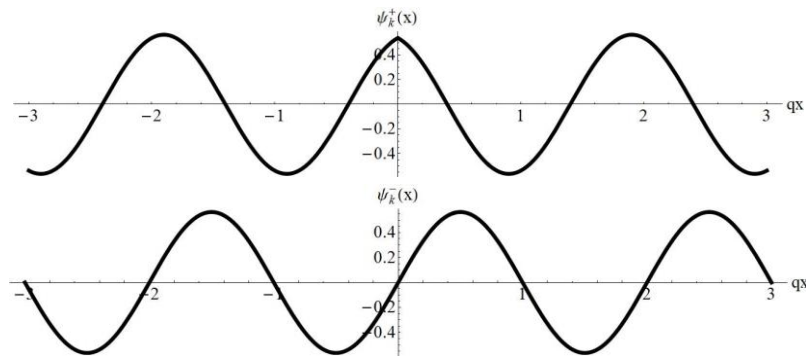


**Figure 6.** Eigenstates of continuous spectrum for the delta potential well corresponding to different eigenvalues of the parity operator: P = +1 from above and P = -1 from below.

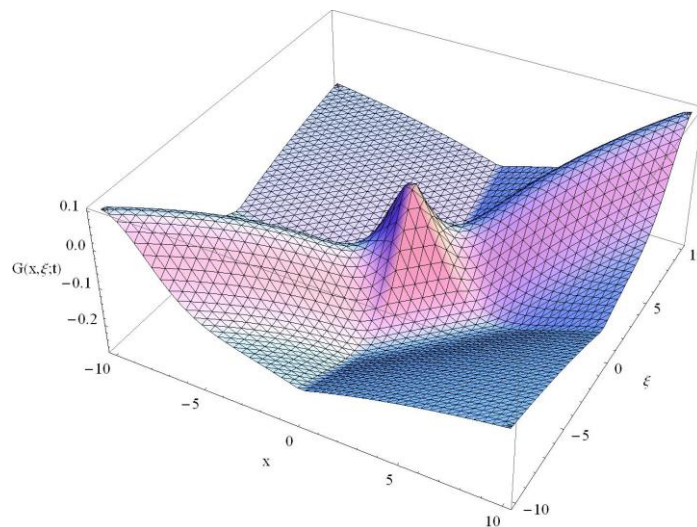


**Figure 7.** Green's function of linear parabolic equation with Dirac delta function source.

#### 4. Wedge shape and measurement of surface diffusion coefficient

This section is devoted to analysis of the simplest solution of the KPZ-equation with delta-functional source and a corollary from it, which is important for physical experiment.

The identity (36) is known to claim that functions (31) and (33) form complete system in the Lebesgue space  $L^2(R)$ . Further, this fact in common with formulae (34) and the expressions:

$$\int_{-\infty}^{+\infty} \psi_k^+(x) \cdot \psi_k^-(x) \cdot dx = 0, \quad \int_{-\infty}^{+\infty} \psi_k^\pm(x) \cdot \psi_0(x) \cdot dx = 0 \tag{42}$$

It means that the phase space  $L^2(R)$  of the infinite-dimensional system (27) can be expanded into the following direct sum:  $L^2(R) = V_0 \oplus V_+^c \oplus V_-^c$ , where  $V_0 \subset L^2(R)$  is its subspace constructed from the single function (31) of the discrete spectrum of ‘energy’  $\varepsilon$  and  $V_\pm^c$  are linear subspaces of  $L^2(R)$  corresponding to the continuous spectrum of this one. Bases of these subspaces  $V_+^c$  and  $V_-^c$  consist from functions  $\psi_k^+(x)$  and  $\psi_k^-(x)$ , respectively.

It is quite hard to deal with eigenfunctions of continuous spectrum, that is why we shall consider the one-dimensional subspace  $V_0$  only. In this case, initial condition for the equation (27) is equal to:

$$\varphi(x, 0) = c_0 \cdot \psi_0(x) \quad (c_0 > 0) \tag{43}$$

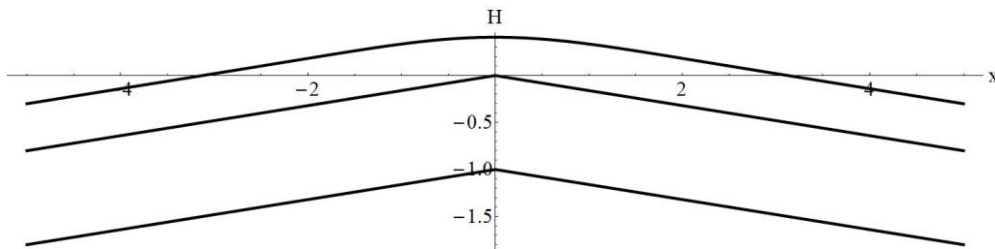


**Figure 8.** Temporal evolution of wedge corresponding to the single state of discrete spectrum: initial shape (from below), shape at  $t = T$  (in the middle) and shape under  $t > T$  (from above).

and the general solution of the equation (27) can be extracted from the formula (20):

$$\varphi(x, t) = c_0 \cdot \psi_0(x) \cdot \exp(\nu \cdot q^2 \cdot t) \quad (44)$$

Applying the Cole-Hopf substitution (7) in opposite direction from (44) we find that:

$$H(x, t) = \left( c + \frac{2 \cdot \nu^2 \cdot q^2}{c} \right) \cdot t + h_0(x), \quad (45)$$

where dependence

$$h_0(x) = \ln(c_0 \cdot \sqrt{q}) - \frac{2 \cdot \nu \cdot q}{c} \cdot |x| \quad (46)$$

is the initial shape of the surface corresponding to initial condition (43) for the auxiliary function (44).

Using formulae (45)-(46) it is easy to check that  $\tan \beta \equiv \left| \frac{\partial H(x, t)}{\partial x} \right| = \frac{2 \cdot \nu \cdot q}{c}$ . Hence, for validity of small angles approximation for the KPZ-equation (14) intensity of the Dirac delta function must satisfy to the next inequality:  $q \ll c/\nu$ . Thus, in this case initial profile (46) is the wedge with the angle near its edge close to  $\pi$ . And according to the expression (45), temporal evolution of the initial condition (46) reduces to the motion of the wedge in vertical direction with constant velocity  $V = c + \frac{2 \cdot \nu^2 \cdot q^2}{c}$ .

This situation is presented in Figure 8.

If under  $t > T$  source of external particles is switched off ( $Q(x) \equiv 0$ ), then the shape of the surface is the following:

$$H(x, T) = h_T - \frac{2 \cdot \nu \cdot q}{c} \cdot |x|. \quad (47)$$

For further considerations it is convenient to assume that  $h_T = 0$ . One can achieve it by choosing  $c_0 = \frac{1}{\sqrt{q}} \cdot \exp \left[ -c \cdot T \cdot \left( 1 + \frac{2 \cdot \nu^2 \cdot q^2}{c^2} \right) \right]$  in the expression (43). In this case, the one-dimensional variant of Eq. (11) gives us the next law of growth of the surface under  $t > T$ :

$$H(x, t) = c \cdot (t - T) \cdot \left[ 1 + \frac{2 \cdot \nu^2 \cdot q^2}{c^2} \right] + \frac{2 \cdot \nu}{c} \cdot \ln \left[ \frac{g(x, t - T) + g(-x, t - T)}{2} \right] \quad (48)$$

where  $g(x, t)$  is the auxiliary function (41). Graph of the function (48) under the fixed time  $t$  is presented in Figure 8. One can observe that under  $t > T$  smoothing of edge of the wedge takes place. If sputtering substance is ideal conductor (at  $t = T$ ), there is a possibility to measure coefficient of surface diffusion  $\nu$  (it is supposed that values  $c$  and  $q$  are known from other measurements).

Let us consider linearly polarized simple harmonic incident electromagnetic wave with complex amplitude  $A \cdot \exp[-i \cdot k \cdot r \cdot \cos(\varphi - \varphi_0)]$ ,  $r$  and  $\varphi$  being polar coordinates in plane  $xz$  and  $k = 2\pi/\lambda$  being wave vector of the wave expressed via its wavelength  $\lambda$ . This wave falls on the wedge (47) from the direction  $(\cos\varphi_0, 0, \sin\varphi_0)$  and gives rise to the wave of horizontal polarization:

$$\vec{E}_H = (0, E(r, \varphi), 0) \quad (49)$$

with the complex amplitude:

$$E(r, \varphi) = A \cdot [u(k \cdot r, \varphi - \varphi_0) - u(k \cdot r, \varphi + \varphi_0 + 2 \cdot \beta)] \quad (50)$$

and to the wave of vertical polarization:

$$\vec{E}_V = \left( \frac{1}{i \cdot k \cdot r} \cdot \frac{\partial H(r, \varphi)}{\partial \varphi}, 0, \frac{1}{i \cdot k} \cdot \frac{\partial H(r, \varphi)}{\partial r} \right), \quad (51)$$

with the complex amplitude of magnetic field:

$$H(r, \varphi) = A \cdot [u(k \cdot r, \varphi - \varphi_0) + u(k \cdot r, \varphi + \varphi_0 + 2 \cdot \beta)]. \quad (52)$$

expressing via the following auxiliary function (see Ref. [20] and references therein):

$$u(\rho, \phi) = \frac{2\pi}{\alpha} \cdot \left[ \frac{J_0(\rho)}{2} + \sum_{l=0}^{\infty} \exp\left(-\frac{\pi \cdot i}{2} \cdot \frac{\pi \cdot l}{\alpha}\right) \cdot J_{\frac{\pi \cdot l}{\alpha}}(\rho) \cdot \cos \frac{\pi \cdot l \cdot \phi}{\alpha} \right] \quad (53)$$

In the formula (53)  $\alpha = \pi + 2 \cdot \beta$  is the angle of the wedge and  $J_\nu(\rho)$  is Bessel function.

Further, one can both measure and calculate using expressions (49)-(53) the specific cross section of this wave:

$$\frac{d\sigma}{d\varphi} = \frac{|\vec{E}|^2}{A^2} \cdot r \quad (54)$$

After that, one can extract the value of the angle of the wedge and, therefore, the value of surface diffusion coefficient  $\nu$  from comparison of experimental and theoretical data.

We underline that in expression (54) the electric field strength  $\vec{E}$  ought to contain reflected wave only. It is obvious that at  $t = T$  series of carbon nanotubes from Figure 4 must be removed from zone of experiment. To simplify formulae (49)-(53), it is suitable to apply both the Sommerfeld ray asymptotics and the Pauli ones [20].

## 5. Conclusion

In this work, the newest research program has been claimed; namely, we have proposed the point of view on nanoengineering as the problem of optimal control by distributed parameter system. We have illustrated this vision by the KPZ-equation (1) describing the growth of a solid state surface, external source of sputtering particles being a control.

We have carried out a number of preliminary investigations in the framework of the suggested research program. In particular, we have constructed the exact solution for the Cauchy problem (14) for the one-dimensional KPZ-equation in approximation of small angles with the source

$Q(x) = \frac{4 \cdot \nu^2 \cdot q}{c} \cdot \delta(x)$  of external particles:

$$H(x, t) = c \cdot t + \frac{2 \cdot \nu}{c} \cdot \ln \left( \int_{-\infty}^{+\infty} G(x, \xi; t) \cdot \exp \left[ \frac{c \cdot h_0(\xi)}{2 \cdot \nu} \right] \cdot d\xi \right) \quad (55)$$

where  $G(x, \xi; t)$  Green's function (37)-(41).

Success in obtaining of the result (55) gives us a confidence that by methods of quantum mechanics [17, 19] we shall construct the exact solution of the Cauchy problem (14) with the following source:

$$Q(x) = \frac{4 \cdot v^2}{c} \cdot \sum_{n=0}^{N-1} q_n \cdot \delta(x - n \cdot b). \quad (56)$$

Function (56) can be physically realized by means of the passing of slow atomic particles through the ‘comb’ with step  $b$  of  $N$  series of carbon nanotubes presented in Figure 4. We underline that intensities  $q_n$  of flows of such particles can be different in different series. Also we stress that carbon nanotubes start to decay at temperature about 1500 K [18]; therefore, these nanostructures can be applied under different kinds of epitaxial procedures.

The suggested in previous section method of surface diffusion coefficient determination is highly realistic, because in work [21] the possibility of the channelling of atomic particles with different masses – from He to Xe – and with energies less than 0.5 keV is theoretically established, metals being among these particles. Moreover, usage of electromagnetic waves scattering data is very fruitful idea, because atomic force microscopy usually presents the shape of the surface under investigation at the beginning and at the end of epitaxial process [4]. But for values like (54) real time measurement can be organized. This information about states of the observed system’s motion may be very important especially for reconstruction of unknown source [7].

It is necessary to emphasize that a wide range of nanotechnological problems can be solved as problems of optimal control by distributed parameter system. For instance, in paper [22] it has been demonstrated that for a multilayer Ge/Si(001) heterostructure with vertically aligned Ge nanoclusters the nonuniform spatial elastic strain distribution gives rise to a three-dimensional potential well for electrons in the strained Si layers surrounding Ge quantum dots. In this situation, elastic strain distribution ought to be considered as a control. And the depth of the potential well ought to be considered as a functional, its maximization resulting in maximization of efficiency of the radiative recombination for the nanostructure [22]. Another example concerns magnetic field controlled domain wall nucleation, pinning and depinning effects in ferromagnetic nanowires [23]. Great attention is paid to these effects to realize magnetic logical cells, which are able to perform main logical operations [23].

On the other hand, scanning probe microscopy gives an opportunity both to create and to investigate nanostructures of different types for various applications [24-26], because nowadays the same device can work as scanning probe lithographer, as atomic force microscope, as magnetic force microscope, and so forth [24-26].

At last, let us remind that Eigler and Schweizer were the first to use a scanning tunneling microscope tip to arrange 35 individual xenon atoms on a single-crystal nickel surface, famously spelling out the letters ‘IBM’ [27]. Thus, nanoengineering and scanning probe microscopy have been closely relating since invention of the second one. And at present, powerful development of functional analysis and computer science is setting the qualitatively new level of this interrelation.

### Acknowledgements

The authors prepared this article during working on the project № 18-08-01356-a of Russian Foundation for Basic Research.

### References

- [1] Ma Z, Zhao M, Qu Z, Gao J, Wang F, Shi Y, Qin L and Liu J 2017 *J. Nanosci. Nanotechnol.* **17** 2213-34
- [2] Mikhailov G M, Fomin L A and Chernykh A V 2017 *Materials* **10** 1156
- [3] Sazanova T S, Otvagina K V and Vorotyntsev I V 2018 *Polym. Test.* **68** 350-8
- [4] Kulikov D A, Potapov A A, Rassadin A E and Stepanov A V 2017 *IOP Conf. Ser.: Mater. Sci. Eng.* **256** 012026
- [5] Kardar M, Parisi G and Zhang Y C 1986 *Phys. Rev. Lett.* **56** 889-92
- [6] Goray L I and Lubov M N 2014 *J. Surf. Invest.* **8** 444-55
- [7] Korotkii A I and Mikhailova D O 2013 *Proc. Steklov Inst. of Math.* **280** 98-118

- [8] Pontryagin L S, Boltyanskii V G, Gamkrelidze R V and Mishchenko E F 1986 *Selected works, v. 4, Classics of Soviet Mathematics, The mathematical theory of optimal processes* (Gordon & Breach Science Publishers)
- [9] Vladimirov V S 1971 *Equations of Mathematical Physics* (Marcel Dekker Inc.)
- [10] Rassadin A E, Stepanov A V and Fomin L A 2018 *Adv. Sci.* **1** 28-33 (in Russian)
- [11] Fursikov A V 2001 *Sb. Math.* **192** 593-639
- [12] Obradovich O, Potapov M M and Razgulin A V 1992 *Comput. Math. & Math. Phys.* **32** 1075-83
- [13] Vasil'ev F P 1970 *USSR Comput. Math. & Math. Phys.* **10** 171-190
- [14] Remizov I D 2018 *Appl. Math. Comput.* **328** 243-6
- [15] Kac M 1949 *Trans. Amer. Math. Soc.* **65** 1-13
- [16] Feynman R P 1953 *Phys. Rev.* **91** 1291-1301
- [17] Landau L D and Lifshitz E M 1977 *Quantum Mechanics: Non-Relativistic Theory* (Pergamon Press)
- [18] Stepanov A V 2015 *J. Surf. Invest.* **9** 789-98
- [19] Galitsky V M, Karnakov B M and Kogan V I 1992 *Problems on Quantum Mechanics* (Nauka) (in Russian)
- [20] Ufimtsev P Ya 2014 *Fundamentals of the Physical Theory of Diffraction* (Wiley-IEEE)
- [21] Dedkov G V 2002 *Surf. Coat. Tech.* **158-159** 75-80
- [22] Yakimov A I, Bloshkin A A and Dvurechenskii A V 2008 *Phys. Rev. B* **78** 165310
- [23] Ermolaeva O L and Mironov V L 2018 *IEEE Trans. Magn.* **54** 1-8
- [24] Huang Z Q, Jiang J J, Hua Y M, Li C Z, Wagner M, Lewerenz H J, Soriaga M P and Anifuso C 2015 *Energy Environ. Focus* **4** 260-77
- [25] Schwager P, Bulter H, Plettenberg I and Wittstock G 2016 *Energy Technol.* **4** 1472-85
- [26] Denning D, Guyonnet J and Rodriguez B J 2016 *Int. Mater. Rev.* **61** 46-70
- [27] Eigler D M and Schweizer E K 1990 *Nature* **344** 524-6